

Chapter 10

In Situ Investigation and Image-Based Modelling of Aluminium Foam Compression Using Micro X-Ray Computed Tomography

Y. L. Sun, T. Lowe, S. A. McDonald, Q. M. Li and P. J. Withers

Abstract Our understanding of the compressive behaviour of foams can be improved by combining micro X-ray computed tomography (CT) and finite element modelling based on realistic image-based geometries. In this study, the cell structure of an aluminium foam (AlporasTM) specimen and its deformation during continuous low-strain-rate compressive loading are recorded by ‘fast’ CT imaging. The original 3D meso-structure is used to construct a 3D finite element model (FEM) for simulation. It is observed that local collapse can occur in cells with a wide variety of shapes and sizes, and the compressive strength is determined by the formation and development of the localised deformation bands. The FE prediction of the stress–strain relationship and cell deformation process has reasonable agreement with the experimental observation, especially for the cell-wall collapse corresponding to the plateau in the stress–strain curve. The simulation also indicates that local yielding actually occurs in cell walls well before the plateau regime. The experimental and image-based modelling methods demonstrated here for foams have potential across a very wide range of applications.

List of Abbreviations

CT Computed tomography
FEM Finite element models

Y. L. Sun · Q. M. Li (✉)
School of Mechanical, Aerospace and Civil Engineering, University of Manchester,
Sackville Street, Manchester M13 9PL, UK
e-mail: qingming.li@manchester.ac.uk

Y. L. Sun
e-mail: sunyonglet1@gmail.com

T. Lowe · S. A. McDonald · P. J. Withers
Henry Moseley X-ray Imaging Facility, School of Materials, University of Manchester,
Manchester M13 9PL, UK

10.1 Introduction

Aluminium foams are ultra-light, multi-functional materials, which have been used widely in various engineering applications, such as sandwich construction and energy absorption. In the last 20 years, the compressive behaviour of foams has been studied by means of macro measurement and phenomenological mechanical models based on idealised cell geometries [1, 2]. However, the meso-scale mechanisms determining the compressive strength have not been completely understood due to the complexity of the cell structures and their deformation.

Recent advances in X-ray computed tomography (CT) enable the non-destructive characterisation of the meso-structure and deformation behaviour of a foam using synchrotron [3] and laboratory X-ray sources [4]. The advantage of CT is its capability to capture the internal structure and deformation of a material in three dimensions (3D). However, one limitation of applying this technique during *in situ* loading is that the test usually has to be interrupted at certain loading stages to allow X-ray scanning. This may introduce stress relaxation and other effects. To overcome this, continuous X-ray CT scanning is used in this study. Moreover, improvements in meshing techniques and the upgrade of computational hardware enable realistic simulations using finite element models (FEM) based on 3D CT images [5]. Such image-based modelling can be applied to isolate the effects of specific physical factors, e.g. cell-wall material properties [6] and strain rate [7], as well as geometrical structural effects. It also can be used to infer the material properties of cell walls using inverse methods [8]. The combination of X-ray *in situ* CT experiments and image-based modelling can provide detailed information for both qualitative and quantitative analyses.

This work aims at investigating the low-strain-rate compression of a closed-cell aluminium foam by *in situ* X-ray testing and image-based modelling. First, *in situ* compression was undertaken during which 3D CT images of the original and successive deformed configurations of the foam were obtained. Then the CT image of the original foam was used as the geometrical basis for a 3D FEM for simulation. The experimental result delineates the deformation mechanism and its effect on the stress–strain relationship of the foam. The numerical prediction provides additional information, e.g. plastic strain distribution in the cell walls.

10.2 Experiment and Modelling

A cylindrical specimen was mechanically cut from a panel of the closed-cell aluminium AlporasTM foam for the *in situ* compression experiment. The diameter and thickness of the specimen are 20 and 10 mm, respectively. The specimen was scanned using a Nikon Metris CT system housed in a customised bay at the Henry Moseley X-ray Imaging Facility (HMXIF, Manchester, UK), which is capable of fast data acquisition useful for minimising blurring during *in situ* experiments.

Radiographs were acquired at an accelerating voltage of 75 kV, a current of 220 μA , a voxel size of 15 μm and an exposure time of 250 ms. A 25 kN Deben rig (Deben Ltd, UK) was used to apply the compressive load. Figure 10.1 shows the schematic of the experimental set-up and a resulting X-ray radiograph (projection). Before loading, 2,000 projections were acquired in order to obtain a high quality CT image to enable accurate meshing of the cell structure for numerical modelling. The sample was then compressed at a loading speed of 0.05 mm/min (strain rate of $8.3 \times 10^{-5} \text{ s}^{-1}$) without interruption when scanning was performed. A smaller number of projections, namely 400 projections, were used for each scan during loading to increase the 3D frame rate. Under these conditions, the displacement of the foam surface attached to the loading platen is 0.083 mm per scan, which corresponds to a compressive strain of 0.83 % and sufficiently preserves the imaging quality under the selected resolution, as verified by the visual inspection of the reconstructed images. Thirty scans were conducted over the whole test and reconstructed into 3D volume data using Nikon Metris CT-Pro reconstruction software. Subsequently, the raw CT data were processed by Avizo standard (Visualization Sciences Group, Bordeaux, France) and grey-level segmentation was used to obtain the 3D images of the solid bodies corresponding to different configurations of the foam specimen under the compression.

The CT image of the original cell structure of the foam specimen was used as the basis for the geometry for the 3D finite element model. A virtual transverse slice of the original foam is shown in Fig. 10.2a, from which the pores (black) and the aluminium walls (white) can be distinguished. By segmenting all the slices, the 3D solid body of the foam (see Fig. 10.2b) was obtained and then meshed using the numerical algorithm in ScanIP (Simpleware Ltd, UK). Figure 10.2c and d show the profile of the created mesh comprising about 14.54 million 4-node tetrahedral elements and 0.94 million 8-node hexahedral elements. It should be noted that the voxel size of the CT images was down-sampled to 60 μm and the internal voids smaller than 100 μm were disregarded in the meshing in order to optimise the element size and thus to reduce the element number. As a result, the relative density of the specimen after image processing and meshing is 17.1 %, which is larger than the 13.5 % measured by the grey value method using original CT volume data and the normal values ranging from 8 to 10 % determined by directly weighing a specimen [2]. The discretized structure was then imported into the general purpose FE code Abaqus to create a finite element model. Two rigid platens were placed on the two ends of the modelled foam specimen, which was compressed by the top platen moving downward at a constant speed with the bottom platen being fixed. No constraint was applied directly to the foam. Abaqus/Explicit was used to perform a quasi-static analysis considering the large deformation and the contact condition neglecting friction. An isotropic elastic perfectly plastic material model was adopted for the cell walls. The elastic modulus, Poisson's ratio and yield strength of the cell-wall material were taken to be 68 GPa, 0.33 and 35.5 MPa, respectively [8].

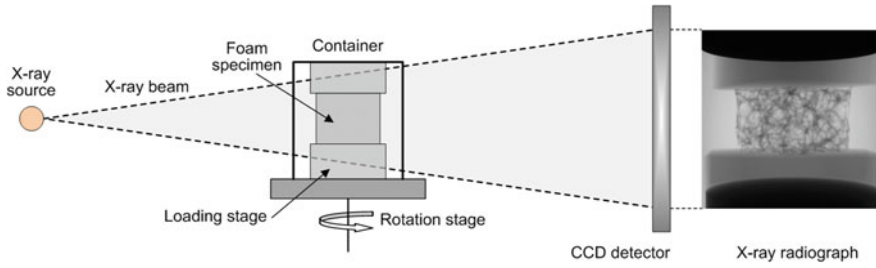


Fig. 10.1 Schematic of the in situ experimental set-up for the foam compression (*left*) and an X-ray radiograph of the scanned foam (*right*)

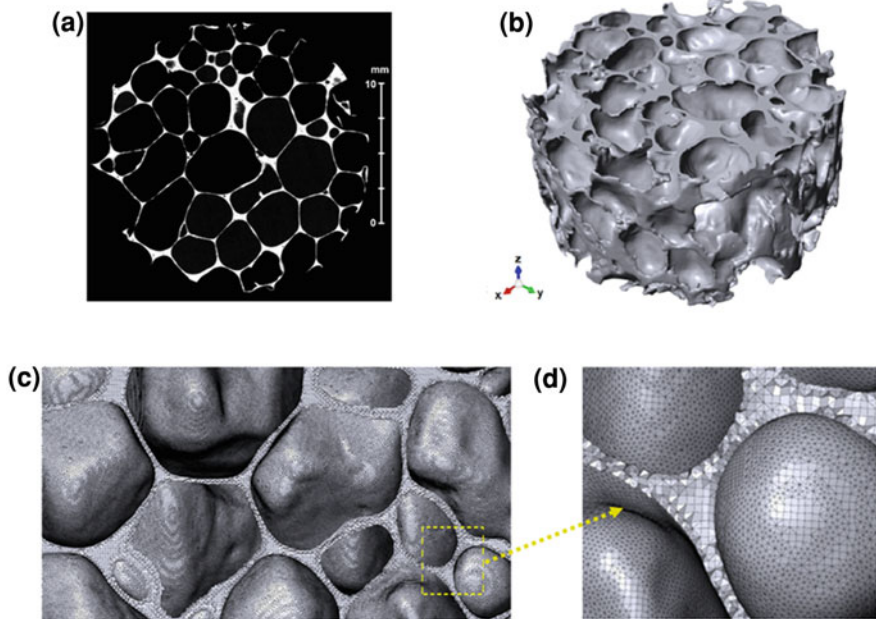


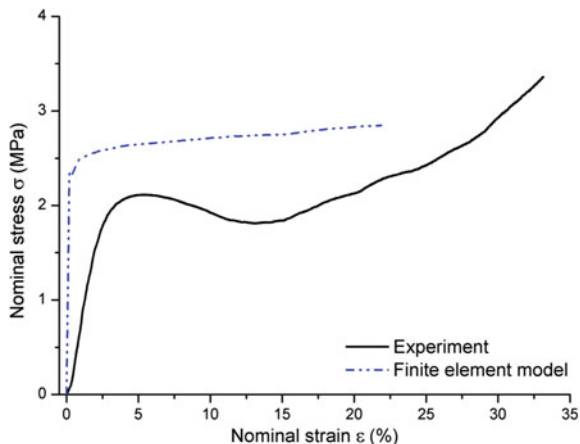
Fig. 10.2 **a** CT slice image in a *transverse plane* of the foam specimen; **b** The 3D image of the foam after the segmentation of the solid portions in the CT volume data; **c** Mesh of the cell structure (view in a *vertical plane*); **d** Enlarged view to show the mesh density

10.3 Results and Discussion

10.3.1 Stress–Strain Relationship

The nominal stress–strain curves obtained from the experiment and simulation are compared in Fig. 10.3. The experimental stress–strain relationship is approximately linear at small strains. However, a nonlinear feature becomes apparent

Fig. 10.3 Experimental and numerical stress–strain curves of the compressed foam



when the stress approaches its maximum during the early compression stage, which is followed by a plateau regime showing prolonged deformation at almost constant stress. After considerably more deformation the stress rapidly rises with strain, reflecting the cell interaction in the densification regime. The numerical prediction generally overestimates the stress level and does not precisely mimic the experimental stress–strain curve. Nevertheless, it successfully captures the essential trend of the stress variation, i.e. the stress almost remains constant in the plateau regime. Unfortunately, the simulation of the densification stage cannot be achieved in the present model due to extensive element distortion associated with the large deformations. The predicted modulus of the linear part of the stress–strain curve is also larger than the experimental one, but is close to the unloading modulus of the same foams measured in previous experiments [9]. The discrepancy between the numerical and experimental results can be attributed to the numerical errors caused by the use of linear elements to discretize the cell walls and possibly an insufficient number of elements over the thin solid walls, as well as the inhomogeneous properties of the cell-wall material [10]. To improve the numerical precision further, more elements would be required which was not possible in this case due to the limited computational power available for over 15 million elements. Furthermore, the increased relative density after meshing and the lack of reliable homogenised material models for the cell walls also hinder more accurate prediction. Nevertheless, the effect of the real meso-scale geometry on the compressive behaviour has been captured in the FE model. Therefore, the current simulation should be regarded as qualitative and capable of providing insights into the compressive behaviour of foams.

10.3.2 Deformation Mechanisms

The foam has an extremely complex cell structure with geometrical imperfections and hierarchical features. From the virtual CT slices shown in Fig. 10.4a and b, it is clearly seen that the cell shape deviates from regular ellipsoids and polyhedra. Moreover, the cell walls themselves are somewhat porous, being significantly thicker at the interconnecting portions. Figure 10.4a and b show the cell deformations within the central cross-section of the 3D volume. The compressive deformation is markedly inhomogeneous, being characterised by the formation and development of localised deformation bands. As the compressive strain increases, some ‘weak’ cells collapse prematurely, presumably due to their inferior load bearing capacity, marking the beginning of localised deformation (see the configuration at a strain of 7.7 % in Fig. 10.4). Deformation then becomes concentrated in these cells which contribute most to the subsequent increase in the compressive strain, indicating the development of a deformation band (see the configuration at a strain of 17.8 % in Fig. 10.4). This process continues until new deformation bands are formed. Such deformation on the cell level corresponds to the plateau regime in the stress–strain curve observed in the macro measurement. Therefore, in common with previous observations [11], the meso-scale cause of the plateau stress, which represents the compressive strength of the foam, is the progressive cell collapse occurring in the localised deformation bands.

The prematurely collapsing ‘weak’ cells play a crucial role in the localised deformation mechanism. However, the exact cause of the premature collapse has not been unequivocally identified. Based on the observation of cell deformation within the cross-section, Bart-Smith et al. [11] identified two critical cell morphologies, i.e. ellipsoidal cells with T-shaped wall intersections and cells with appreciably curved walls, for the weak cells, but these morphologies cannot be easily distinguished in the present experimental observations. Our results reveal that the weak cells susceptible to collapse actually have a wide variety of shapes and sizes. Consequently, existing simple (mostly 2D) geometric criteria are unlikely to describe them, especially when their 3D nature is considered. It is questionable whether a 2D geometry can describe the 3D cell structure of a foam, since the 2D geometric characteristics of one foam cell may change significantly from one cross-section to another. For instance, a ‘small cell’ observed in one cross-section may be part of a large cell and the 2D curvature does not necessarily represent the 3D one. Therefore, the observation of 3D cell deformation is important in establishing a better understanding of the local collapse behaviour.

The deformation bands in the central XZ and YZ planes are shown in Fig. 10.4a and b as the dotted lines. The comparison between them indicates that the location and orientation of the bands depend on the plane selected. The band in the XZ plane is close to the top and is slightly inclined. By contrast, the band in the YZ plane is closer to the bottom and is significantly inclined. The cells outside the bands essentially retain their original shape, even when the compressive strain has reached 17.8 %. To inspect the 3D features of these deformation bands, translucent

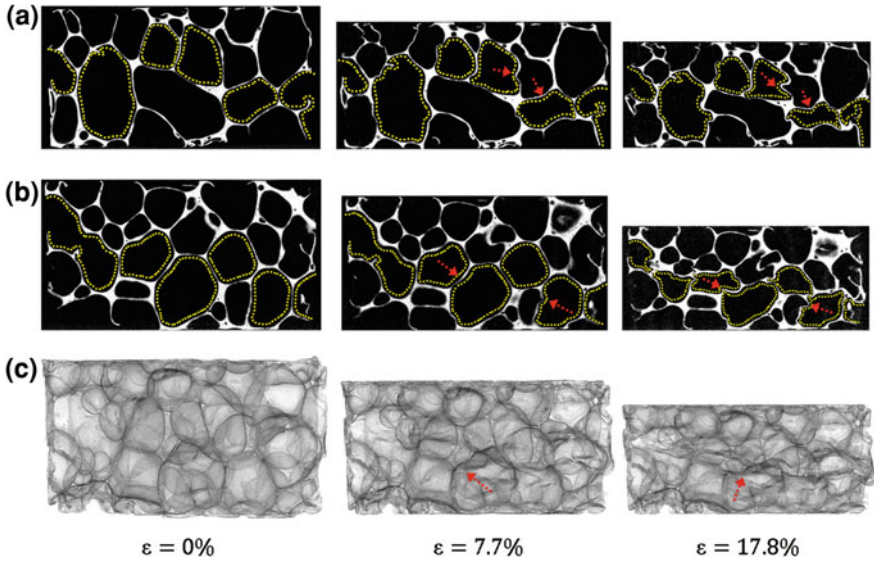


Fig. 10.4 Configurations of the foam specimen at different nominal strains: **a** Cross-section in the central XZ plane; **b** Cross-section in the central YZ plane; **c** Translucent foam body to show the 3D deformation of internal cells. The *dotted lines* indicate the cells in the localised deformation bands and the *arrows* indicate the collapse modes of cell walls

images of the foam body are presented and compared, as shown in Fig. 10.4c. It is evident that shear deformation across cells is dominant on the cell level, see the cells indicated by the arrows in Fig. 10.4c, whereas both bending and buckling occur at the smaller scale associated with cell walls, see the portions indicated by the arrows in Fig. 10.4a and b.

It reveals that the load distribution across the cells is very complicated even when the foam is subjected to uniaxial compression. The 3D deformation of two centrally located cells is shown in Fig. 10.5 and complex morphological changes are clearly seen. These cross-sectional and 3D observations confirm that premature cell collapse depends not only on the cell morphology but also on the actual load the cell experiences.

Figure 10.6 shows a comparison between the experimental observation and the numerical prediction. It is seen that the FE model predicts well the cell deformation, including the location and mode of the collapse of cell walls. Some fine features may be lost in the simulation because of the limited precision of the reconstruction and the meshing. Nevertheless, the simulation captures the essential deformation mechanisms and allows further computational analysis. For instance, the equivalent plastic strain distribution in the cell walls can be obtained from the simulation, and it indicates that extensive plastic deformation has already occurred in some locations at a strain of 0.5 %, as shown in Fig. 10.7, which is well before the plateau stage is reached. Such local yielding at small strain is probably the

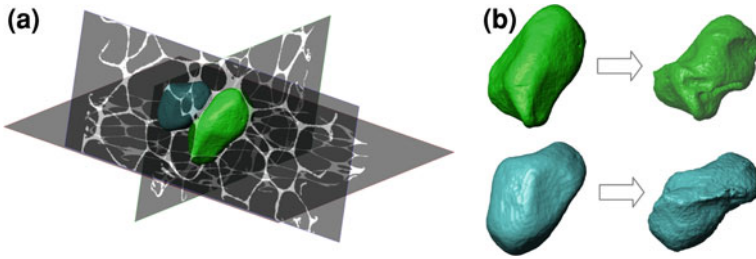


Fig. 10.5 **a** Two typical cells located in the centre of the foam specimen; **b** 3D deformation of the central cells at a strain of 12.0 %

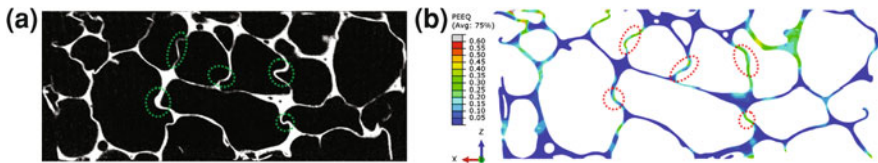


Fig. 10.6 Comparison of the cell deformation in the central XZ plane at a strain of 17.8 %: **a** Slice image from CT data; **b** Numerical result (contour of the equivalent plastic strain in the deformed configuration). The extensively deformed local portions of the cell walls are indicated by the dotted ellipses

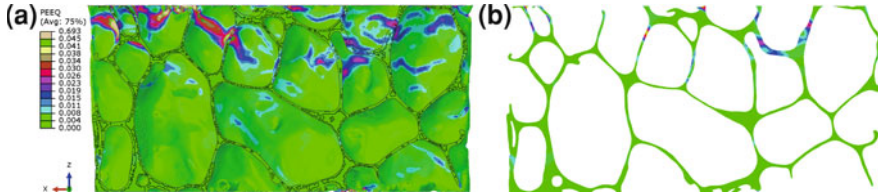


Fig. 10.7 Plastic strain distribution in the cell walls at a strain of 0.5 %: **a** Half of the solid body viewed in the Y direction; **b** Cross-section in the central XZ plane

cause of the discrepancy between the tangent modulus and unloading modulus of the linear part of the stress–strain curves observed in previous experiments [9].

10.4 Conclusions

In situ X-ray compression and image-based modelling are used to investigate the low-strain-rate compressive behaviour of a closed-cell aluminium foam. According to the experimental observation, the compressive strength is mainly determined by cell collapse in the localised deformation bands. The CT images reveal

that some cells exhibit premature collapse due to morphological effect and complex load distribution, and both bending and buckling occur in the walls of the 'weak' cells having various shapes and sizes. The finite element simulation based on the real cell structure extracted from CT images predicts the stress–strain curve and cell deformation in a reasonable agreement. The numerical prediction can be improved by developing a more reliable material model for the cell walls and reducing numerical errors associated with the meshing. The simulation indicates that significant local yielding occurs well before the plateau regime is reached.

Acknowledgments The authors would like to acknowledge the assistance given by the IT Services and the use of the Computational Shared Facility at The University of Manchester. The supports from the Engineering and Physical Science Research Council (EPSRC) grants EP/F007906/1 and EP/F028431/1 and Royal Society grant JP100958 are also acknowledged. The first author is grateful for the PhD scholarship from the School of Mechanical, Aerospace and Civil Engineering, The University of Manchester.

References

1. Gibson L.J., Ashby, M.F.: Cellular Solids: Structure and Properties. Cambridge University Press, Cambridge (1997)
2. Ashby, M.F., Evans, A.G., et al.: (2000) Metal Foams: a Design Guide. Elsevier, Netherlands
3. Maire, E., Babout, L., et al.: Recent results on 3D characterisation of microstructure and damage of metal matrix composites and a metallic foam using X-ray tomography. *Mater. Sci. Eng. A* **319–321**, 216–219 (2001)
4. McDonald, S.A., Mummery, P.M., et al.: Characterization of the three-dimensional structure of a metallic foam during compressive deformation. *J. Microsc.* **223**(2), 150–158 (2006)
5. Young, P.G., Beresford-West, T.B.H., et al.: An efficient approach to converting three-dimensional image data into highly accurate computational models. *Philos. Trans. R. Soc. A: Math. Phys. Eng. Sci.* **366**(1878), 3155–3173 (2008)
6. Jeon, I., Asahina, T., et al.: Finite element simulation of the plastic collapse of closed-cell aluminum foams with X-ray computed tomography. *Mech. Mater.* **42**(3), 227–236 (2010)
7. Vesenjajk, M., Veyhl, C., et al.: Analysis of anisotropy and strain rate sensitivity of open-cell metal foam. *Mater. Sci. Eng. A* **541**, 105–109 (2012)
8. Jeon, I., Katou, K., et al.: Cell wall mechanical properties of closed-cell Al foam. *Mech. Mater.* **41**(1), 60–73 (2009)
9. Andrews, E., Sanders, W., et al.: Compressive and tensile behaviour of aluminum foams. *Mater. Sci. Eng. A* **270**(2), 113–124 (1999)
10. Simone, A.E., Gibson, L.J.: Aluminum foams produced by liquid-state processes. *Acta Mater.* **46**(9), 3109–3123 (1998)
11. Bart-Smith, H., Bastawros, A.F., et al.: Compressive deformation and yielding mechanisms in cellular Al alloys determined using X-ray tomography and surface strain mapping. *Acta Mater.* **46**(10), 3583–3592 (1998)